Biochimica et Biophysica Acta 1837 (2014) 315–325

Contents lists available at ScienceDirect

Biochimica et Biophysica Acta

journal homepage: www.elsevier.com/locate/bbabio

Action spectra of photosystems II and I and quantum yield of photosynthesis in leaves in State 1

Agu Laisk [a,*], Vello Oja [a], Hillar Eichelmann [a], Luca Dall'Osto [b]

[a] Tartu Ülikooli Molekulaar- ja Rakubioloogia Instituut, Riia tn. 23, Tartu 51010, Estonia
[b] Università di Verona, Dipartimento di Biotecnologie, Strada Le Grazie, 15 37135 Verona, Italy

ARTICLE INFO

Article history:
Received 27 September 2013
Received in revised form 30 October 2013
Accepted 3 December 2013
Available online 12 December 2013

Keywords:
Leaves
Photosystems
Excitation partitioning
Quantum yield
Electron transport

ABSTRACT

The spectral global quantum yield (Y_{II}, electrons/photons absorbed) of photosystem II (PSII) was measured in sunflower leaves in State 1 using monochromatic light. The global quantum yield of PSI (Y_I) was measured using low-intensity monochromatic light flashes and the associated transmittance change at 810 nm. The 810-nm signal change was calibrated based on the number of electrons generated by PSII during the flash ($4 \cdot O_2$ evolution) which arrived at the PSI donor side after a delay of 2 ms. The intrinsic quantum yield of PSI (y_I, electrons per photon absorbed by PSI) was measured at 712 nm, where photon absorption by PSII was small. The results were used to resolve the individual spectra of the excitation partitioning coefficients between PSI (a_I) and PSII (a_{II}) in leaves. For comparison, pigment–protein complexes for PSII and PSI were isolated, separated by sucrose density ultracentrifugation, and their optical density was measured. A good correlation was obtained for the spectral excitation partitioning coefficients measured by these different methods. The intrinsic yield of PSI was high ($y_I = 0.88$), but it absorbed only about 1/3 of quanta; consequently, about 2/3 of quanta were absorbed by PSII, but processed with the low intrinsic yield $y_{II} = 0.63$. In PSII, the quantum yield of charge separation was 0.89 as detected by variable fluorescence F_v/F_m, but 29% of separated charges recombined (Laisk A, Eichelmann H and Oja V, Photosynth. Res. 113, 145–155). At wavelengths less than 580 nm about 30% of excitation is absorbed by pigments poorly connected to either photosystem, most likely carotenoids bound in pigment–protein complexes.

1. Introduction

In oxygenic photosynthesis the two photosystems (PSII and PSI) operate in series during the transport of electrons from H_2O to CO_2. This implies a serious constraint on the antenna systems serving these photosystems, since turnover by the two photosystems must be equal in the white light that the photosynthetic system is adapted to utilize (more details in Discussion). This would not be a problem if the quantum efficiency of electron transport and pigment composition of the antennae were equal in both photosystems. Recent advances in molecular analysis of the photosynthetic antenna systems have revealed the numbers of Chls bound with different pigment–protein complexes (Table 1). For example, assuming a typical PSII dimer composition of $C_2S_2M_2$ (two cores, two strongly and two medium bound LHC) and taking monomer density ($½C_2S_2M_2$) of 1.2 μmol m^{-2} and PSI density of 1 μmol m^{-2}, then there are 173 μmol Chl m^{-2} associated with monomeric PSI and 175 with monomeric PSII, resulting in the ratio of excitation partitioning between PSII and PSI, $a_{II}/a_I = 1.01$. In case of an extremely large PSII antenna, including two loosely bound LHCII per dimer ($C_2S_2M_2L_2$) and the same center densities 1.2 and 1 μmol m^{-2}, then there are 173 μmol Chl m^{-2} associated with PSI and 226 with PSII, resulting in $a_{II}/a_I = 1.3$.

Based on these analytically measured antenna sizes per PSII and PSI monomer, excitation partitioning between the photosystems is proportional to the ratio of the densities of photosystems. The latter generally indicates the dominance of PSII, varying from 2.5/1 to 1.2/1 depending on growth light quality in pea [1,2]. Based on excitation spectra of low-temperature PSI fluorescence, excitation partitioning to PSI was estimated to be only 0.3 in bean leaves over the visible range, with peaks approaching 0.5 at some wavelengths [3], indicating significant over-excitation of PSII in relation to PSI. Recently the excitation balance of the two photosystems was explored in relation to the quantum yield of CO_2 fixation in cucumber leaves grown under the sunlight spectrum or under shade light (preferentially exciting PSI) or blue light (preferentially exciting PSII) [17]. The relative excitation capture rates of the two photosystems, PSII/(PSI + PSII), calculated in vivo from Chl fluorescence and leaf transmittance signals at 810 nm, were strongly proportional to

Abbreviations: A/D, analog-to-digital converter; Car, carotenoids; Chl, chlorophyll; ETR, electron transport rate; FRL, far-red light; GL, green light (540 nm); LED, light-emitting diode; LHCI, LHCII, light-harvesting complexes of PSI and PSII; PAD, PFD, photon flux density, absorbed and incident; PC, plastocyanin; PQ(H_2), plastoquinone (reduced); PSI, PSII, photosystems I and II; P700, donor pigment of PSI; STF, single turnover flash; WOC, water-oxidizing complex; Y_{II}, Y_I, global quantum yield of the photosystem with respect to all quanta absorbed by the leaf; y_{II}, y_I, intrinsic quantum yield of the photosystem with respect to quanta absorbed by the particular photosystem

* Corresponding author. Fax: +372 742 0286.
E-mail address: alaisk@ut.ee (A. Laisk).

0005-2728/$ – see front matter © 2013 Elsevier B.V. All rights reserved.
http://dx.doi.org/10.1016/j.bbabio.2013.12.001

Table 1
Pigment content in subcomplexes of PSI and PSII [4–16].

	Chl *a*	Chl *b*	Chl (*a* + *b*)	b-Car	Lut	Neo	Viol
PSI core	106		106	5			
PSI gap	3.5	2.5	6				
Lhca(1/4)	22.8	7.2	30	1	2.7		1.3
Lhca(2/3)	24.7	6.3	31	1.5	2.5		1
PSI composition							
LHCI	51	16	67	2.5	5.2		2.3
PSI-LHCI	157	16	173	7.5	5.2		2.3
PSI-LHCI-LHCII	181	34	215	7.5	11.2	3	5.3
PSII core	35		35	11			
Lhcb1…3	8	6	14		2	1	1
Lhcb4 (CP29)	6	2	8		1	1	1
Lhcb5 (CP26)	6	3	9		1	1	1
Lhcb6 (CP24)	5	5	10		1		1
PSII composition							
LHCII (S,M,L)	24	18	42		6	3	3
C_2	70		70	22			
C_2S_2	142	46	188	22	16	10	10
$C_2S_2M_2$	200	92	292	22	30	16	18
$C_2S_2M_2L_2$	248	128	376	22	42	22	24

the same ratio calculated from in vitro antenna size and photosystem density values, but the proportionality constant was about 1.3 in favor of the in vitro data.

If there are problems with balancing the two photosystems, the condition should be reflected in the action spectrum of photosynthesis [18]. The first report of unbalanced stimulation of PSI and PSII was the Emerson enhancement effect, when addition of short wavelength (PSII) light synergistically enhanced the quantum yield of photosynthesis under far red (PSI) light [19]. Subsequent measurements revealed a characteristic drop in photosynthetic quantum yield at 450–500 nm [20–22], suggested to be caused by over-excitation of PSII relative to PSI due to absorption by Chl *b* [23]. Instead of the physical spillover [24], in plants the partitioning of excitation is regulated toward an optimum by the "state transition" mechanism, which is the ability to redistribute LHCII between PSII and PSI depending on excitation spectral composition [2,25,26]. Thus, though the total numbers of Chls are closely similar per photosystem and the most striking difference between PSII and PSI is in terms of the Chl *a*/*b* ratio and carotenoid content, in leaves the number of trimeric LHCII may be variable dependent on growth conditions, leaving the actual antenna sizes of PSII and PSI, as well as the excitation partitioning ratio, open.

In this work we revisit the problem of photosystem excitation balancing, making use of recent advances in optical and O_2 evolution measurements on leaves. We report the action spectra of PSII and PSI separately in terms of the global yield (with respect to all absorbed quanta) and analyze the intrinsic quantum yields (with respect to quanta exciting the particular photosystem) and excitation partitioning between the photosystems. In the blue part of the spectrum both photosystems are screened by pigments whose spectrum is similar to that of carotenoids. In accordance with the early results with *Chroococcus* and *Chlorella* [27] and with cucumber leaves [17,20] this shows that excitation is not transferred efficiently from all carotenoids to Chl in leaves.

2. Materials and methods

2.1. Plant material

Sunflower (*Helianthus annuus* L.) plants were grown in 4-l pots in nutrient-enriched soil in a growth chamber (AR-95HIL, Percival, from CLF Plant Climatics GmbH, Emersacker, Germany) at a PFD of 450 μmol quanta m^{-2} s^{-1}, 14/10 h day/night cycle, 25/20 C temperature, and 70% relative humidity. Fully expanded, attached leaves of 3 to 4 week-old plants were used in experiments. Leaves of *Betula pendula*, *Ulmus glabra* and *Aegopodium podagraria* were collected from plants growing outdoors and, with petioles in water, used in experiments.

2.2. Leaf chamber and illumination

A laboratory-made two-channel leaf gas exchange measurement system (Fast-Est Instruments, Tartu, Estonia) enabled control of CO_2, H_2O and O_2 pressures and measurement of O_2 evolution and transpiration. The leaf was enclosed in a 32-mm diameter by 3-mm deep chamber and flushed with gas at a flow rate of 0.5 mmol s^{-1}. To stabilize leaf temperature and immobilize the leaf for optical measurements, the upper epidermis was sealed with starch paste to a glass window in contact with a water jacket. Gas exchange occurred through the lower epidermis. The leaf temperature was always within 0.2 °C of the water jacket temperature (22 °C).

The leaf chamber was illuminated via a branched fiber-optic light guide. Plastic fibers (1 mm, Toray Polymer Optical Fiber, PF series, from Laser Components, Gröbenzell/München, Germany) were individually arranged to produce uniform illumination of the chamber-enclosed adaxial leaf surface from three superimposed light sources. In this work one branch was used for FR illumination (LED 720-66-16100, Roithner Lasertechnik GmbH) and the second branch for additional green light (OD-520 L, Opto Diode Corp.). The third branch was connected to a STF source (Machine Vision Strobe MVS-7020, EG&G Optoelectronics, Salem, MA) or, alternatively, to a white LED (Enfis UNO Array 5 × 5 neutral white 4000–4500 K) equipped with selected interference filters (when the absolute quantum yield of PSII was measured).

The quantum yield of PSI was measured with non-saturating single-turnover flashes (STF) generated by the Xe source via interference filters (10 nm band-width at half-height, ThorLabs, Newton, NJ). Quantum energy input, either integrated over time for flashes (μmol photons m^{-2}) or as quantum flux rate of filtered white LED light (monochromatic, μmol photons m^{-2} s^{-1}), was measured by a Miniature Fiber Optic Spectrophotometer PC 2000 (Ocean Optics, Dunedin, FL), spectrally calibrated against a 1000 W FEL type etalon lamp, model 63350 serial No. 7-1074, according to manufacturer's instructions. Photon absorption by the leaf during a flash (μmol m^{-2}) was calculated by multiplication of the filtered flash emission spectrum for leaf absorptance spectrum. The actual spectrum of the "monochromatic light" was calculated as the product of the emission spectrum of the light source and the transmission spectrum of each filter. At some wavelengths this significantly shifted the effective midpoint of the band.

2.3. Measurement of light absorption in the leaf

Leaf absorptance was measured with the PC 2000 using a leaf disk placed in an integrating sphere and illuminated by white light from a halogen source. The integrating sphere was home-made, internal surface of 8.5 cm diameter was made of compressed white Teflon powder. In the center of the sphere there were an object and reference holder side by side—a white horizontal metal sheet with two holes of 13 mm diameter. Light was guided into the sphere from the bottom by a single fiber, arranged so that most of the light cone passed through the object hole. Two pairs of recordings were made for one measurement. The fraction of stray light not illuminating the sample was measured, first, placing a black object on the sample holder and leaving the neighbor reference holder empty (reading R_1) and, second, leaving the sample holder empty and placing the black body on the reference holder (R_2). The fraction of stray light, $T_{black} = R_1 / R_2$ was about 0.04. With leaf samples, first, a 15 mm leaf disk was placed on the sample holder and another, 15 mm white Teflon disk on the reference holder (R_3), and then the places of the leaf and Teflon disk were exchanged (R_4). The corresponding leaf scattering signal $T_{leaf} = R_3 / R_4$. Leaf absorptance (A) was calculated as

$$A = \frac{1-T_{leaf}}{1-T_{black}}. \quad (1)$$

Along with photosynthetically active pigments, a small part of radiation was absorbed in cell walls and other non-pigment structures. We assumed that at 800 nm all absorption was non-photosynthetical and spectrally constant. Therefore, absorptance in photosynthetic pigments (A_P) was found as

$$A_P = A \cdot \left[1 - \frac{\ln(1-A_{800})}{\ln(1-A)}\right], \quad (2)$$

where parameters A and T in Eqs. (1) and (2) are wavelength dependent over the spectrum.

2.4. Measurement of PSI fluorescence

Non-variable fluorescence of PSI, typically $0.37F_0$ in the long-wave spectral window of 750 ± 20 nm, was calculated as the invariable part of F_0 fluorescence present in the long-wave window, but absent in the short-wave window of 680 ± 10 nm. In overnight dark-adapted leaves fluorescence was measured in the two wavelength windows in the F_0 and F_m states. The 750 nm signal was plotted vs. the 680 nm signal, a straight line was drawn through the two measured points and extrapolated to zero of the 680 nm signal. The obtained offset at 750 nm was considered to be PSI fluorescence [48,49].

2.5. O_2 evolution measurements

Oxygen evolution was measured in the flow-through gas exchange measurement system with a calcium-stabilized zirconium O_2 analyzer (S-3A, Ametek, Pittsburgh, PA, USA) on a background of 80 ppm O_2 in N_2 and 200 ppm CO_2. The analyzer was calibrated against the atmospheric O_2 concentration. The calibration has been confirmed by the ratio of O_2/CO_2 fluxes of 1.0055 during photosynthesis in high light [28]. Due to the small volume of the leaf chamber and tubing, the half-response time of the system was only 0.6 s [29]. For steady-state measurements the reference (zero) was recorded after darkening the leaf. Respiratory O_2 consumption was strongly suppressed due to the low ambient O_2 concentration [30]. Density of PSII centers was measured as 4 · O_2 evolution generated by an individual saturating STF [57].

2.6. 810 nm transmittance measurements

Leaf transmittance at 810 nm was measured with a laboratory-made modulated spectrophotometer [31]. A 810-nm LED (Type ELD 810-525, Roithner Lasertechnique, Vienna, Austria), filtered by a 40-nm band-pass interference filter (FB 800-40, ThorLabs), is driven by rectangular pulses of 5.5 μs at 90 kHz by a quartz-stabilized generator. The beam is applied to a 2-cm^2 sub-area of the leaf surface. A fiber bundle collects transmitted radiation from the abaxial side of the leaf and guides it to a sensor PIN diode (S3590-01, Hamamatsu, Japan). An FB 800-40 band-pass interference filter (ThorLabs) minimizes the sensitivity to Chl fluorescence and non-modulated radiation. The PIN diode is operated under a constant counter-voltage of 10 V minimizing and stabilizing the internal capacitance of the diode. The photocurrent is amplified by a feedback controlled current-to-voltage converter, rectified, offset against 2 V, and the difference is further amplified.

2.7. Calculation of the redox state of P700

In these calculations the 810-nm signal was scaled to be 0 at complete oxidation (saturation pulse) and 1.0 at complete reduction (dark). The value of the 810-nm signal during pre-illumination was defined s. From the condition of equilibrium [31,32]

$$\frac{P700}{P700^+} = k_E \frac{PC}{PC^+}, \quad (3)$$

where the reduced fractions P700 and PC were assumed to generate the positive optical signal. A quadratic equation describes the redox ratio r = P700 / P700$^+$:

$$r = \frac{-B + \sqrt{B^2 - 4AC}}{2A}, \quad (4)$$

where

$$A = 1-s; B = \frac{k_E \varepsilon}{\varepsilon + p} + \frac{p}{\varepsilon + p} - s(1 + k_E); C = -sk_E, \quad (5a, b, c)$$

and $\varepsilon = 4$, which is the ratio of extinction coefficients of P700 and PC at 810 nm, p is the ratio of PC/P700 in leaves (typically 2) determined from the oxidative titration of PSI donors by FRL [32,33] and $k_E = 30$ is the P700/PC equilibrium constant [31,32]. The redox state of P700 is

$$\frac{P700}{P700 + P700^+} = \frac{r}{1 + r} \quad (6)$$

and the number of donor side electrons, per PSI, is

$$n_e = \frac{r}{1 + r} + \frac{rp}{r + k_E}. \quad (7)$$

2.8. Membrane isolation, pigment–protein complexes purification and pigment analysis

Stacked thylakoids were isolated from sunflower leaves as previously described [34]. Membranes corresponding to 400 μg Chl were washed with 5 mM EDTA and then dissolved in 800 μl of 0.7% α-DM, 10 mM Hepes, pH 7.5. Dissolved samples were then fractionated by ultracentrifugation in a 0.1 to 1 M sucrose gradient containing 0.06% α-DM and 10 mM Hepes, pH 7.5 (22 h at 280,000 g, 4 °C). Green bands corresponding to monomeric Lhcb, trimeric LHCII, PSII core and PSI + LHCI complexes [35] were harvested. Absorption spectra were obtained in 10 mM Hepes, pH 7.5, 0.06% α-DM, and 0.2 M sucrose; measurements were performed using an SLM-Aminco DW-2000 spectrophotometer at room temperature. Pigments were extracted from complexes with 85% acetone buffered with Na_2CO_3, and then the supernatant of each sample was recovered after centrifugation (15 min at 13,000 g, 4 °C).

3. Results

3.1. General strategy

We seek to determine the intrinsic quantum yields (electrons transported per photon absorbed by the particular photosystem), y_{II} and y_I of PSII and PSI, respectively, and likewise the excitation partitioning coefficients a_{II} and a_I between PSII and PSI in leaves. To achieve the goals, we apply recent advances in studies of the photosynthetic electron transport in leaves—fast-response measurements of O_2 evolution for PSII responses and precise 810 nm transmittance measurements for PSI responses. The spectrum of the global quantum yield of PSII, Y_{II} (electrons transported per all quanta absorbed by the leaf) was determined by measuring the O_2 evolution rate under rate-limiting intensities of different wavelengths of monochromatic light. The global yield of PSI, Y_I, was determined by comparison of the responses of PSII (O_2 evolution) and PSI (the corresponding 810 nm transmittance response) to low-intensity flash illumination. The intrinsic yields of PSI (y_I) and PSII (y_{II}, electrons transported per photon absorbed by the photosystem) were determined by solving a system of equations, based mainly on the fact that in far-red light the intrinsic quantum yield of PSI, y_I, is close to the global yield Y_I, as most photons are absorbed by PSI at these wavelengths (corrections were considered by measurements at two wavelengths). The obtained very high yield y_I = 0.88 leads to a conclusion that a small amount of antenna Chl is

needed to support the measured global yield Y_I, while the larger part of Chls are joined with PSII. Despite of it, the measured global yield Y_{II} was still relatively low, revealing the intrinsic quantum yield of PSII, $y_{II} = 0.63$, which is significantly lower than the yield of charge separation of 0.89, detected from Chl fluorescence.

3.2. Action spectrum of PSII from O_2 evolution

The global quantum yield of PSII oxygen evolution, Y_{II}, was measured using weak monochromatic light. The leaf was pre-illuminated in far-red light (FRL, 706 nm, 198 μmol m^{-2} s^{-1}), 200 ppm CO_2 and 2% O_2 concentration in N_2. Under this illumination PC was completely oxidized and P700 was only little reduced, as indicated by the 810 nm transmittance signal. PQ was also oxidized due to the strong over-excitation of PSI. For the measurement of quantum yield, first, the gas was changed to 80 ppm O_2 and the 200 ppm CO_2 and after 2 min the pre-illumination FRL was changed to a monochromatic light cut from the spectrum of a white LED by interference filters. The intensity of the light was chosen such that the rate of O_2 evolution did not change much compared to that under FRL (intensities of 10 to 20 μmol m^{-2} s^{-1} dependent on wavelength). Fig. 1 shows a typical response of the O_2 evolution rate to a transition from the pre-illumination to the monochromatic measurement light. Oxygen evolution, initially supported by PSII excitation due to the pre-illumination light, rapidly changed dependent on the intensity of the monochromatic light (adjusted such that O_2 evolution only slightly increased at the wavelength of 462 nm in Fig. 1), stabilized for a second, and then linearly declined in the light with the rate that differed depending on excitation wavelength. It was checked that – with the baseline for O_2 measurements recorded in the dark – the rate of O_2 evolution was proportionally related to the intensity of the monochromatic light. Light-induced changes in respiratory O_2 uptake were minimized due to the very low background O_2 concentration, which strongly suppressed the respiratory O_2 uptake [30], and due to the fast-response measurements, eliminating slow readjustments in respiratory metabolite pools. Therefore, the global quantum yield Y_{II} was calculated as 4 times the initial (at 2.7 s, Fig. 1) O_2 evolution rate under the monochromatic light, divided by the monochromatic PAD. The later linear decline was caused by the accumulation of PQH_2 due to over-excitation of PSII at this wavelength, as indicated by fluorescence rise (below). In terms of e^- per photon absorbed in the leaf, the global PSII yield, Y_{II}, was 0.42–0.43 in red and green light, but decreased to about 0.30 in the blue spectral range (Fig. 2). As anticipated, at wavelengths >680 nm the yield decreased rapidly.

Chlorophyll fluorescence was slightly above F_0 during pre-illumination, but decreased to the F_0 level when pre-illumination was turned off without the transition to the monochromatic light. When the pre-illumination light was changed to monochromatic light, fluorescence slowly and linearly increased in parallel with the decreasing O_2 evolution rate. The quantum yield of PSII charge separation, $(F_m - F) / (F_m - F_{PSI})$ was 0.89 in the beginning of the monochromatic illumination, considering PSI fluoresce as indicated in the figure. The gradual decline in O_2 evolution rate and increase in Chl fluorescence yield following the application of the monochromatic light indicated over-excitation of PSII in relation to PSI at this wavelength, leading to accumulation of PQH_2. The relative difference in O_2 evolution rate, [(initial rate − rate after 3 s) / initial rate], showed a complex action spectrum with maxima in the blue and red (Fig. 3). This result indicated that the two photosystems were not balanced indeed, but PSII was over-excited compared to PSI in blue and red light. We further investigated the quantitative extent of the misbalance in PSII and PSI excitation.

3.3. Optical flash-responses from PSI and PSII

Measurement of the global PSI yield, Y_I, was more complicated than that of Y_{II}, since no gas exchange signal could be directly related to activity of this photosystem. Information about PSI performance was extracted from the leaf transmittance change at 810 nm, which reports on the reduction state of P700 and PC, the primary and secondary electron donors to PSI.

In these experiments the leaf was pre-illuminated under combined green plus far-red light (GL, 540 nm, 18 μmol m^{-2} s^{-1} × 0.72 absorption, plus FRL, 706 nm, 40 μmol m^{-2} s^{-1} × 0.62). Under these conditions PQ at the PSII acceptor side and PC at the PSI donor side were almost completely oxidized, but P700 was about half-reduced, being in redox-equilibrium with PC [31]. The pre-illumination was terminated and immediately followed by a weak monochromatic STF from the filtered Xe source.

The flash-induced 810-nm signal changes were small compared to the full amplitude of the 810-nm signal (Fig. 4). A correction for Fd^- signal, 15% of the oxidation jump, was considered for the complete oxidation level, because Fd becomes reduced, decreasing the overall optical signal

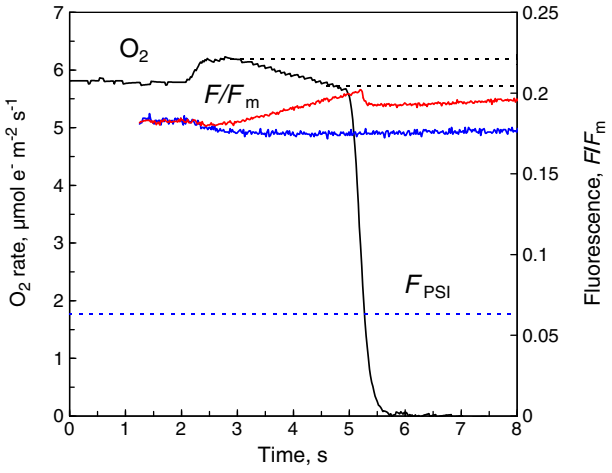

Fig. 1. Measurement of the global quantum yield of PSII, Y_{II}. A sunflower leaf was pre-illuminated under FRL, 706 nm, 198 μmol m^{-2} s^{-1} (incident) · 0.401 (absorptance), 200 ppm CO_2 and 2% O_2 concentration in N_2, and transferred for 3 s to 462 nm light, 24.3 · 0.909 μmol m^{-2} s^{-1}, followed by darkness. The initial O_2 evolution (5.8 μmol e^- m^{-2} s^{-1}, black line) was supported by PSII excitation by FRL; increase in O_2 evolution at 2 s indicates the change in illumination from FRL to blue light. Chl fluorescence was recorded by PAM-101 fluorometer in parallel with the light quality transition (red line) or the preillumination FRL was just turned off without the change to the blue light (blue line). Notice the decrease in O_2 evolution (black dotted lines) and increase in fluorescence under the blue light, caused by the accumulation of PQH_2. Dotted line F_{PSI} indicates the level of PSI fluorescence.

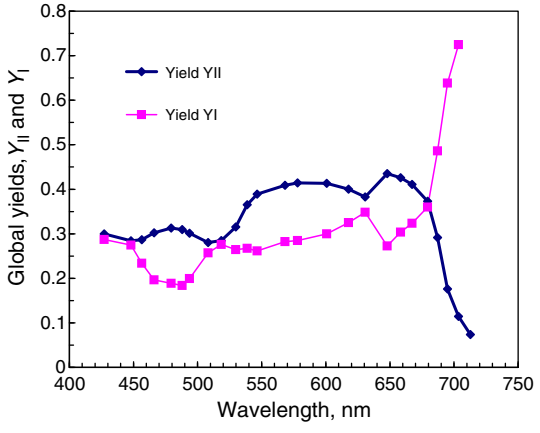

Fig. 2. Spectra of the global quantum yields (with respect to quanta absorbed in the leaf) of PSII, Y_{II}, obtained from the initial O_2 evolution rate after the change from FRL to different monochromatic light, and of PSI, Y_I, obtained from the flash-induced 810 nm transmittance change calibrated at different wavelengths.

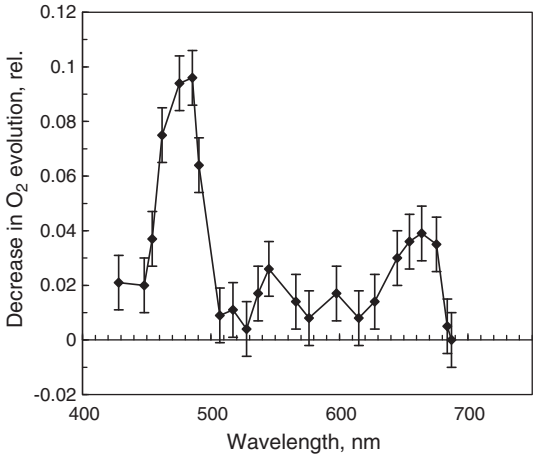

Fig. 3. Relative decrease in O_2 evolution during the 3 s exposure (difference between the black dotted lines, Fig. 1) after the change from FRL to light of different wavelengths.

as soon as the donor side carriers PC and P700 become oxidized. Under the pre-illuminating GL + FRL light the steady-state equilibrium reduction of P700 was supported by linear electron flow from PSII excitation [36] and by the "dark re-reduction" of inter-photosystem carriers [37], which probably occurs via the same pathway as the fast, proton-uncoupled component of cyclic electron transport around PSI [33,38]. These electron transport pathways continued operation for some time in the dark after the background illumination was terminated, causing post-illumination reduction of $P700^+$ and PC^+, shown as the reference line measured by darkening the leaf without the flash (Fig. 4). In the exemplified recording a 650 nm weak STF was applied immediately after the background light was turned off. The difference between the measurement and reference traces represents the temporal response of the 810-nm signal to electron flow generated by the STF alone.

Fig. 5 illustrates the post-flash time course of this 810 nm difference signal in detail, an average over a large number of measurements. Clearly there is a delay of about 2 ms between the PSI flash-induced oxidation of the P700↔PC equilibrium pair and the following PSII-induced reduction of these carriers, leaving sufficient time to separate the 810 nm optical responses from PSI and PSII electrons. The initial reduction state of P700 was between 0.4 and 0.5 in individual leaves, corresponding to a very small fraction of reduced PC (as illustrated in Fig. 4). As a result, the post-flash re-equilibration of the PC↔P700 pair was fast and invisible in our recording, so the arriving PSII electrons were clearly distinguished from the PSI-induced oxidation of the donor side carriers. The statistics of electron transfer from flash-reduced PQ through Cyt b_6f to PC↔P700 rather exactly followed the Poisson (exponential) temporal kinetics with an average time constant of about 12 ms (but somewhat different in individual leaves).

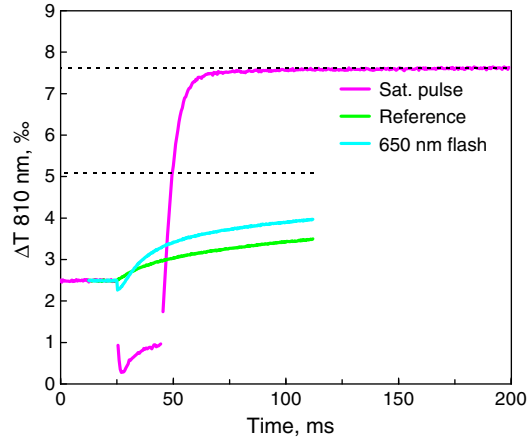

Fig. 4. Scaling of the 810-nm signal. The leaf was pre-illuminated with green light (GL, 540 nm, 18 μmol m^{-2} s^{-1}) plus far-red light (FRL, 706 nm, 40 μmol m^{-2} s^{-1}). In this state a strong saturation pulse (7000 μmol m^{-2} s^{-1}, 20 ms) was applied for determining signal levels corresponding to the complete oxidation (in the beginning of the pulse, $\Delta T = 0$) and complete reduction ($\Delta T = 7.6‰$ after the pulse) of PSI donor side (dotted line at $\Delta T = 5.1‰$ indicates the conditional transition level from the oxidation of P700 to the oxidation of PC). The $\Delta T = 0$ level was corrected for the signal by Fd^-, assumed to be 15% of the P700 oxidation jump. For measurements, the background GL + FRL was turned off and a weak STF (650 nm) was immediately applied. A reference transient indicating PSI reduction by PSII during preillumination plus dark reduction by equivalents from the PSI acceptor side was measured by terminating the illumination without the flash.

3.4. Per electron response of the 810 nm signal and PSI density

For an individual leaf the (flash–reference) difference signals are shown in Fig. 6 for 650 and 713 nm wavelengths. The post-flash immediate response towards oxidation is the principal measure of the quantum yield of PSI at the flash wavelength, but for further analysis it had to be converted from ‰ of the optical signal into electrons m^{-2}, in order to be compared with the amount of absorbed photons m^{-2}. The full amplitude of the exponential reducing phase was a good measure for the calibration of the optical signal, proportional with the amount of electrons generated by PSII during the flash (but overestimated by a small portion of the flash-transferred electrons cycling back from the acceptor side of PSI, see below).

Initially the PSI cycle was neglected and the 810-nm signal change was calibrated based on the known quantity of PSII electrons generated by the STF. The latter was calculated from the known amount of photons in the STF, multiplying the flash photon dose (assuming 7% loss due to double hits) by the global quantum yield of PSII (Fig. 2). This procedure resulted in a variable per electron signal (for brevity we use this term instead of μmol e^- m^{-2}) dependent on flash wavelength (Fig. 7), indicating an evident correlation between the 810-nm per electron signal and leaf absorbance (apparent optical density). For an individual leaf the scattering of data was small and we obtained a strong non-linearly saturating dependence of the 810-nm per electron signal vs. leaf absorbance. The curve (Fig. 8) approached a saturating value at the absorbance of 0.6, the minimum in the green spectral area, but the data point measured at 713 nm – the extreme low values of absorbance and of the PSII yield – significantly jumped up from the smooth curve, indicating that the number of electrons arriving at the PSI donor side was underestimated. On this basis we assumed that not only PSII electrons caused the exponentially rising signal, but a fraction of electrons transferred to the PSI acceptor side by the flash cycled back to the donor side with temporal kinetics rather similar to those of the PSII electron transfer

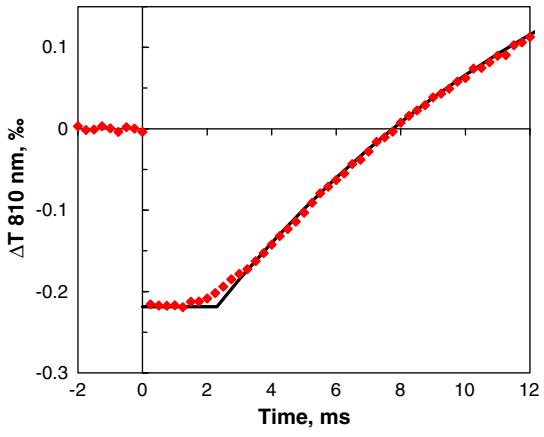

Fig. 5. Time-resolved response of the 810-nm transmittance signal to a low-intensity STF. The flash causes immediate oxidation of PSI donors. After a delay of 2 ms the donor pool is reduced by electrons arriving from PSII. Data points are the average of 200 recordings fitted to an exponential function (black line).

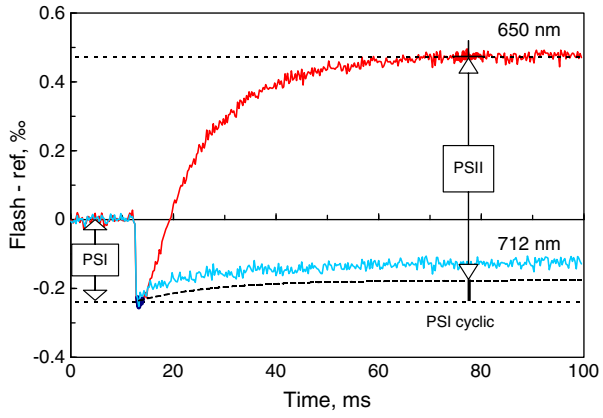

Fig. 6. Responses of PSI and PSII electron transport to a weak STF. The leaf was pre-stabilized at GL + FRL as in Fig. 4, the pre-illumination light was turned off and a 650 nm STF was immediately applied. For reference, the same procedure was repeated without the flash. The difference "flash–reference" shows the response of the 810-nm signal, first oxidation due to PSI electron transport and then reduction due to PSII → PSI electron transport. Upper (red) curve, response to a 650 nm flash; lower (blue) curve, response to a 713 nm flash. Cycling of 15% of the flash-transferred electrons back to the donor side was determined as explained in Fig. 8 and the signal caused by these electrons is indicated by the black dashed line.

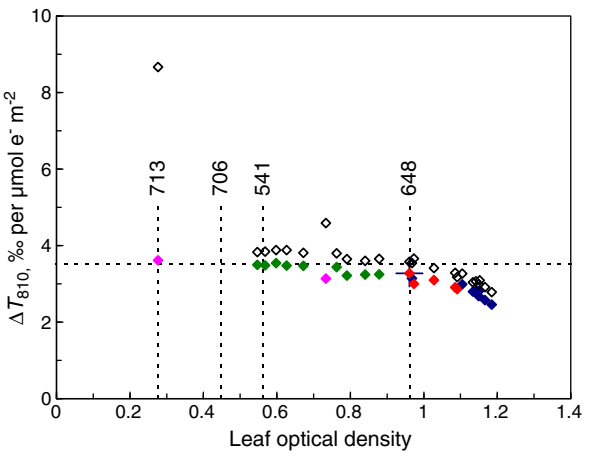

Fig. 8. Nonlinear correlation between the 810 nm signal sensitivity and leaf absorbance. Empty data points were measured neglecting cycling of flash-transferred PSI electrons. Then different cycling proportions were assumed (the same at all wavelengths), until the smoothest curve was obtained assuming 15% of the flash-transferred electrons cycled back to the donor side. Colors of data points approximate the color of the flash light. Figures at vertical lines indicate wavelengths chosen for leaf preconditioning (706 and 541) and wavelengths used in Eqs. (12) and (13) (713 and 648).

through the Cyt b_6f complex [38]. Inserting different values for the proportion of cycling electrons, the smoothest curve over the whole spectrum was obtained on an assumption that 15% of electrons, transferred to the PSI acceptor side by the flash, cycled back to the donor side at all flash wavelengths (Fig. 8). The PSI cyclic flow had little influence on the results at wavelengths, where PSII produced many electrons per flash, but the influence was significant in far-red, where the contribution of PSI cyclic electron flow was about equal to the contribution of PSII electrons (Fig. 6).

The dependence of the 810 nm per electron signal on leaf optical density is evidently based on inhomogeneous flash excitation across the leaf interior. Blue and red photons were strongly absorbed in the leaf layers close to the upper surface. 810 nm photons sensing the oxidized P700 had a greater chance to escape from the leaf when the oxidized PSI centers were concentrated at the leaf surface. In green and far-red light the generated $P700^+$ was rather equally distributed across the leaf. As a result the strongly scattering 810 nm sensing beam, having a lesser chance to escape from deeper sites in the leaf, could visit every $P700^+$ several times. During the measurement of the maximum signal, P_m, all PSI centers were oxidized, thus, there was no gradient of $P700^+$. Comparing the flash-oxidation signals with the P_m deflection we considered the different intra-leaf gradient by applying a normalization coefficient for the measured 810 nm deflection, extending from 1.0 for green and far-red light to 1.5 for blue light, as seen from the relative trend of the per electron signal in Fig. 8. Now, by comparison of the normalized 810 nm flash signal with the total 810 nm P_m signal we converted the relative optical signal to the relative number of electrons per PSI, involved in the flash oxidation–reduction procedure (Eq. (7)). As an example, we revealed that for the 650 nm flash, the amount of 0.199 μmol e^- m^{-2} generated by PSII was equivalent to 0.186 electrons per PSI. This pair of figures allowed us to calculate the density of PSI, which was 0.199/0.186 = 1.07 μmol m^{-2}. Thus, knowing the absolute number of flash-generated electrons m^{-2} by PSII on the one hand, and knowing the fraction of PSI these electrons reduced on the other hand, we obtained the density of PSI centers. Before the absorbance-dependent normalization of the 810 signal, the so obtained PSI density was variable dependent on wavelength of the flash, but remained constant after the signal was normalized to the most uniform intra-leaf distribution of $P700^+$. Considering that in this leaf the PSII density was 1.76 μmol m^{-2} (measured as $4 \cdot O_2$ evolution generated by saturating STF), the PSII/PSI ratio was 1.76/1.07 = 1.64.

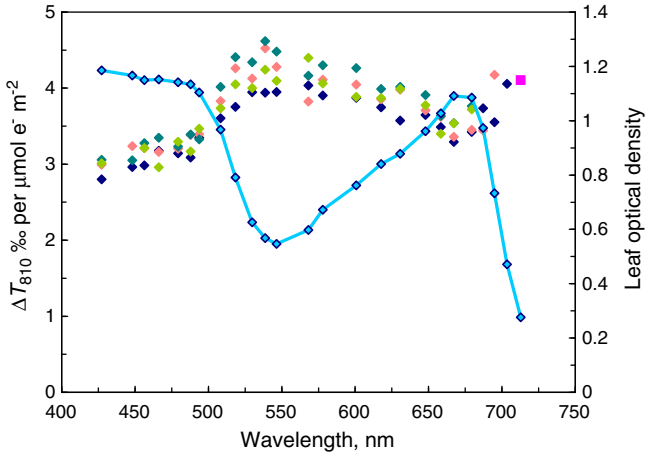

Fig. 7. Spectral dependence of the 810-nm signal sensitivity, Δ*T*, in ‰ per μmol e^- m^{-2} in PSI donors. Typical leaf absorbance (optical density) is shown for comparison. Data from four sunflower leaves are indicated by different colors.

3.5. Global quantum yield of PSI

For finding the global quantum yield of PSI, the relative number of electrons transferred per PSI was first multiplied by PSI density, μmol m^{-2}, for finding the number of electrons transferred by PSI per m^{-2} of leaf. Further, the quantum efficiency of PSI electron transport was found by dividing the amount of transferred electrons by the dose of photons in the flash, μmol m^{-2}. However, the so obtained figure characterizes the efficiency of those PSI, which had P700 reduced when the flash was applied. The global quantum yield of all PSI with their P700 reduced was found by dividing the above fractional yield by the fraction of PSI with reduced P700, calculated from Eq. (6) for the pre-conditioning light. The so calculated global quantum yield of PSI with reduced P700, Y_I, is presented in Fig. 2 in comparison to the global quantum yield of PSII.

The result of Fig. 2 confirms the initial result of Fig. 3, indicating significant over-excitation of PSII in some spectral intervals. The global PSI yield, Y_I, is generally lower than the PSII yield Y_{II}, as shown in

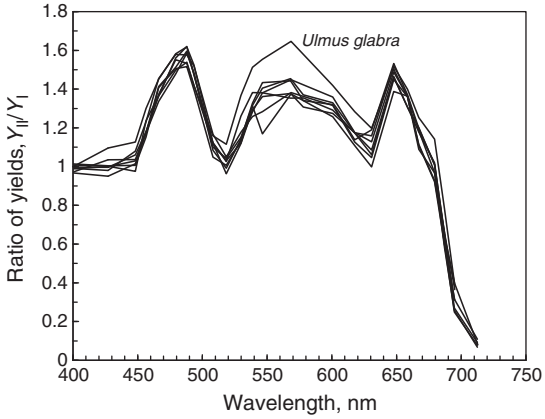

Fig. 9. Ratio of the quantum yields of PSII and PSI, Y_{II}/Y_I, for four sunflower (*Helianthus annuus*) leaves grown in the laboratory and leaves collected from the yard of the laboratory (*Ulmus glabra*, *Betula pendula* and 2 leaves of *Aegopodium podagraria*).

Fig. 9, which summarizes measurements for different leaves growing in- and outdoors. Over wavelength ranges of 470 to 500 nm, 540 to 580 nm, and 640 to 650 nm the Y_{II}/Y_I ratio rises to 1.5–1.6. Only at 400 to 450 nm, and 510, 620 and 680 nm does the Y_{II}/Y_I ratio approach unity, drastically decreasing at wavelengths >680 nm and approaching the limit of resolution at 710–720 nm. The results were practically identical for leaves grown in the growth chamber or outdoors, except that the green maximum of PSII yield tended to be higher in *U. glabra*, a very thick dark-green leaf.

We again emphasize that the yields in the ratio Y_{II}/Y_I are not the quantum yields of electron transport of PSII and PSI with respect to photons exciting the corresponding antenna systems, but global yields that were calculated with respect to all absorbed quanta. Therefore, the Y_{II}/Y_I ratio encompasses the intrinsic quantum yields of the photosystems, as well as the partitioning ratio of photons between the photosystems. In the following analysis we shall resolve excitation partitioning between, and intrinsic electron transport efficiency of, the individual photosystems.

3.6. Intrinsic yield with respect to partitioned photons

For analysis of excitation partitioning between the photosystems we proceeded from an evident relationship, valid for both photosystems,

$$Y = a \cdot y, \tag{8}$$

where Y is the measured global quantum yield with respect to total absorbed light, a is excitation partitioning (capture) coefficient by the particular photosystem and y is the intrinsic yield with respect to photons captured by this photosystem. To find the true intrinsic yields of PSI and PSII we used an additional budget condition, considering that in the red part of the spectrum only photosynthetically active pigments, Chl *a* and Chl *b* absorb light:

$$a_I + a_{II} = \frac{Y_I}{y_I} + \frac{Y_{II}}{y_{II}} = 1, \tag{9}$$

from which we obtain

$$y_{II} = \frac{Y_{II}}{1 - \frac{Y_I}{y_I}}. \tag{10}$$

This relationship (Eq. (10)) is valid for any wavelength, provided that the intrinsic quantum yields y_I and y_{II} do not vary with excitation wavelength and photosynthetically inactive pigments are absent. Defining the wavelengths as λ_1 and λ_2, we write

$$y_{II} = \frac{Y_{II\lambda 1}}{1 - \frac{Y_{I\lambda 1}}{y_I}} = \frac{Y_{II\lambda 2}}{1 - \frac{Y_{I\lambda 2}}{y_I}}, \tag{11}$$

yielding

$$y_I = \frac{Y_{II\lambda 1} \cdot Y_{I\lambda 2} - Y_{II\lambda 2} \cdot Y_{I\lambda 1}}{Y_{II\lambda 1} - Y_{II\lambda 2}} \tag{12}$$

and

$$y_{II} = \frac{Y_{I\lambda 1} \cdot Y_{II\lambda 2} - Y_{I\lambda 2} \cdot Y_{II\lambda 1}}{Y_{I\lambda 1} - Y_{I\lambda 2}}. \tag{13}$$

These expressions contain only measured global quantum yields on the right side. One wavelength was chosen at 713 nm, where $Y_{II} = 0.074$ and $Y_I = 0.776$ (Fig. 2). For better contrast the second wavelength was chosen at 648 nm, where PSII activity was high and the global yields were $Y_{II} = 0.435$ and $Y_I = 0.273$. Substituting these values into Eqs. (12) and (13) we obtained the intrinsic yields $y_I = 0.88$ and $y_{II} = 0.63$.

3.7. Partitioning of excitation between PSII and PSI

The above determined intrinsic yields allowed us to calculate the spectral excitation partitioning coefficients

$$a_I(\lambda) = \frac{Y_I(\lambda)}{y_I} \quad \text{and} \quad a_{II}(\lambda) = \frac{Y_{II}(\lambda)}{y_{II}}, \tag{14, 15}$$

presented in Fig. 10. Characteristically, in the green and red spectral range PSII received about 0.65–0.68 but PSI only 0.32–0.35 of absorbed photons. A confirmation for our calculation routine came from the fact that applying Eq. (9) for different wavelengths the sum $a_I + a_{II}$ remained constant with $y_I = 0.88$ and $y_{II} = 0.63$ over the whole amber-red spectral range, where carotenoids did not absorb light.

In the blue spectral range the sum $a_{II} + a_I$ declined from unity, showing that about 30% of light was screened by photosynthetically inactive pigments, correspondingly reducing the availability of photons for photosynthesis.

For comparison with the in vivo kinetic data, pigment–protein complexes were isolated from a sunflower leaf and separated by sucrose

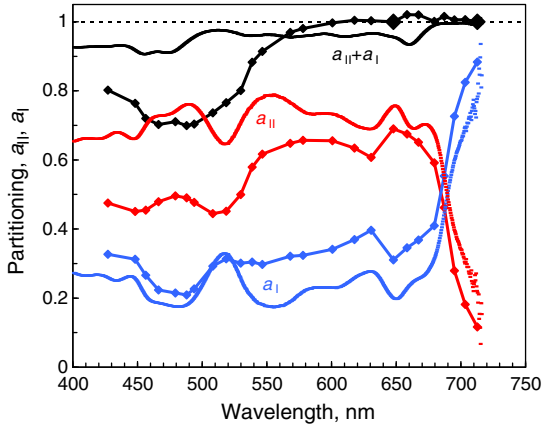

Fig. 10. Excitation partitioning coefficients to PSII, a_{II}, (red) and to PSI, a_I, (blue) calculated using the intrinsic quantum yields, $y_{II} = 0.63$ and $y_I = 0.88$ (curves with data points indicated every 10 nm). Relative optical densities of PSII + LHCII and PSI + LHCI separated in sucrose density gradient are presented as continuous curves. Black curve is the sum $a_{II} + a_I$; the two larger diamonds indicate data points used for calculation of y_{II} and y_I from Eqs. (12) and (13).

gradient ultracentrifugation as described in the Methods section. The absolute absorbance of pigments bound with PSII was significantly higher than the absorbance of pigments bound with PSI (Fig. 11). The fractional absorbance of the PSII core plus total Lhcb (denoted PSII + LHCII) was only a little higher than the functional in vivo excitation partitioning coefficient to PSII, a_{II}, at the red maximum of Chl absorption (Fig. 10). The fractional absorbance of PSI pigments was still rather significantly less than the calculated partitioning coefficient a_I in the red part of the spectrum. A distinct difference between the absorbance of the pigment complexes and excitation partitioning to photosystems was evident at the short-wave end of the spectrum. At wavelengths <580 nm the functional excitation partitioning to both PSII and PSI dropped by up to 30%, but this was not reflected in absorbance of the pigment complexes.

4. Discussion

In our hands the sum of the global quantum yields $Y_{II} + Y_I$ was about 0.42 + 0.30 = 0.72 in the red part of the spectrum (Fig. 2), equivalent to 0.125 · 0.72 = 0.090 O_2 per photon absorbed by the leaf. This value is somewhat lower than 0.106, reported for net O_2 evolution of 37 C_3 species [39], but close to the yields of CO_2 uptake of 0.073 to 0.093 in C_3 plants under non-photorespiratory conditions [40–44]. We note that the measurements [39] were carried out with incandescent illumination deprived of the far-red part by short-pass filters, and measured with the LiCor quantum sensor. The latter has a very sharp cutting edge exactly at 700 nm, but most short-pass filters leave significant shoulder of transmittance from 700 to 720 nm, still active in photosynthesis [45]. As a result, in these measurements the photosynthetically active PAD was underestimated in the near far-red region, resulting in overestimated quantum yield (see also Fig. 12).

4.1. Charge recombination in PSII

Our kinetic analysis shows interesting spectral details, but generally it confirms the significant over-excitation of PSII compared to PSI in intact leaves, pre-illuminated with dominantly PSI light in our experiments. This raises the question of how electron transport is balanced for the two photosystems operating in series. Both photosystems are linked by linear electron flow, J_L, from H_2O to CO_2 and alternative acceptors (the latter being mainly N and O_2, [46]). Consequently, J_L must be equal through both photosystems. In addition to the linear flow, both photosystems may operate with losses, first, due to excitation decay before charge separation, second, charge recombination (or electron cycling) after charge separation, such that their total excitation

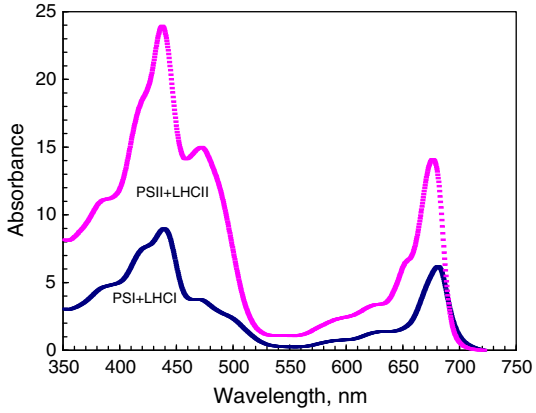

Fig. 11. Spectral absorbance of PSII core + LHCII (red line) and PSI core + LHCI (blue line), separated in sucrose density gradient. Membranes corresponding to 400 μg of chlorophylls were dissolved and separated by ultracentrifugation; green fractions were collected and the optical density of each fraction was measured (presented on the ordinate axis as the optical density per cm of spectrophotometer cuvette, recalculated assuming 1 ml of solvent).

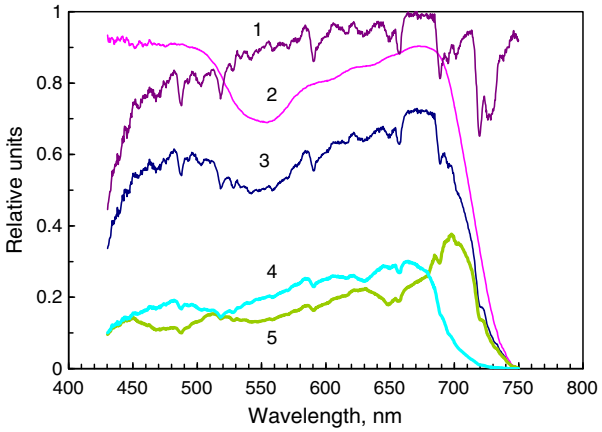

Fig. 12. Importance of near infrared light in photosynthesis. The photon density spectrum of direct + diffuse sunlight was measured at midday (curve 1). Considering leaf absorptance (curve 2) the spectrum of photon flux density absorbed by the leaf was found (curve 3). The rate of PSII (curve 4) and PSI (curve 5) electron transport was calculated for low monochromatic light intensities considering the global quantum yields Y_{II} and Y_I (Fig. 2).

conversion rate is $J_{II} = J_L + J_{CII}$ and $J_I = J_L + J_{CI}$, where the subscripts CII and CI indicate the decay/recombination/cycling rates in PSII and PSI. In this conceptual framework we focus on the low-light conditions used for the measurements of the quantum yield, where J_C involves physiological pathways of cyclic electron transport (ms time domain), recombination processes involving separated charges (μs time domain) and the F_0 fluorescence-emitting process of excitation decay before charge separation (ps time domain), but no non-photochemical excitation quenching (NPQ).

In absence of losses the total quantum yield of the 2-photosystem mechanism could be $Y_{II} = Y_I = 0.5$ e^- per photon absorbed, but in our hands the yields were $Y_{II} = 0.42$ and $Y_I = 0.30$ in the red light (Fig. 2). Furthermore, our analysis succeeded in specifying that such a low global yield was mainly caused by significant losses of excitation energy in PSII, operating with an intrinsic efficiency $y_{II} = 0.63$ with respect to photons partitioned to this photosystem, while PSI operated with a higher yield $y_I = 0.88$. In our analysis y_I and y_{II} were found from a system of equations based on measurements at two wavelengths, one of which was chosen such where PSI activity dominated, and the other such where PSII activity dominated. Then the excitation partitioning coefficient a_I was found such that it ensured the measured global yield Y_I and a_{II} was found such that it ensured the measured global yield Y_{II}. Since the system of equations was derived on an assumption that the sum $a_I + a_{II} = 1$, the latter condition was a priori fulfilled at the two wavelengths chosen for determination of y_I and y_{II}. Correctness of the calculation method was confirmed by the fulfillment of the condition $a_I + a_{II} = 1$ at other wavelengths in the red part of the spectrum, where carotenoids did not absorb light (Fig. 10).

Intrinsic yields of the photosystems are of central importance for finding the excitation partitioning coefficients. The value of $y_I = 0.88$ is in good agreement with the value of 0.96 ± 0.11, determined on PSI trimer complexes from *Synechocystis* 6803 using the pulsed photoacoustic method [47]. In accordance with the high intrinsic yield, a relatively low excitation partitioning coefficient a_I satisfies the measured global yield Y_I. Consequently, most Chl is connected with PSII, in accordance with the PSII/PSI center density ratio of 1.64, obtained from our analysis.

It has been suggested that the excess of PSII centers over PSI centers is justified by the inevitable photoinhibition of PSII, as a result of which electron transport rates through both photosystems get balanced when about a half of PSII are inactivated [50]. In our experiments leaves were not exposed to high light intensities, eliminating the possibility of photoinhibition, thus the investigated state was an uninhibited natural

state of the photosynthetic machinery. At the low dominantly PSI light the quantum yield of charge separation in PSII was 0.89, as detected by the variable fluorescence F_v/F_m (considering F_{PSI} in the total F_0), but 29% of separated charges did not yield in O_2 evolution, resulting in the intrinsic yield of 0.63. The reason for the low yield, not accompanied by high fluorescence, could be charge recombination from an acceptor side carrier [51]. Such recombination did not occur from Q_A^-, since it was not noticed in DCMU inhibited leaves [52], but rather charges recombined from a reduced form of Q_B [53]. This mechanism decreases the efficiency of PSII electron transport, but has no influence on the F_0 and F_m values reflecting charge separation, maintaining the F_v/F_m ratio constant.

Our finding of a low PSII yield in steady state at low light is in conflict with insignificant "misses" of excitation (<10%) for the advancement of S-states [54]. Evidently, the low-yield state of PSII is not a principal property of this photosystem, but is adjusted in intact leaves during photosynthesis. The high yield of S-state advancement has been shown not for single photons, but mainly for saturating STFs (multiple repeated excitation during a few μs), and not in leaves, but in algae and chloroplasts at low physiological temperatures and optimally adjusted pH values. Misses increase with increasing temperature and acidity of the medium. In our intact sunflower leaves during the slow light-limited photosynthesis at 22 °C chloroplast stroma was acidified by accumulating 3-phosphoglyceric acid [55,56]. Lumenal space surrounding WOC was even more acidic in relation to the stroma due to water-splitting plus proton transport through Cyt b_6f—though probably not much during the slow photosynthesis, but sufficiently to exceed the threshold for ATP synthesis. As a result of lumen acidification the quantum efficiency of S-state advancement could decrease. Because of this TyrZ on the PSII donor side remained oxidized longer after each primary charge separation, thereby facilitating radiationless charge recombination. In accordance with this model, the period-4 oscillations of flash-induced O_2 evolution are damped rather rapidly in leaves, indicating a high probability for "misses"; for example, in dark-adapted sunflower leaves O_2 evolution was about equal from the 3rd and the 4th flashes [57]. The hypothetical pH-based mechanism of regulation needs further investigation, but our present and recent results clearly show that in leaves during photosynthesis the actual quantum yield of PSII electron transport is inhibited or down-regulated to be lower than indicated by Chl fluorescence parameters.

4.2. Carotenoids screen blue light

A prominent feature of the action spectra of the photosystems was the blue drop of about 30% at wavelengths <550–580 nm. Early measurements of the photosynthetic action spectrum in the green alga *Chlorella* exhibited a similar drop. This phenomenon was related to screening by carotenoids absorbing blue light [20,58]. More information about excitation transfer from Car to Chl was obtained from "sensitized fluorescence" spectra, indicating a 40–50% excitation transfer efficiency in green algae [59], no transfer from xanthophylls but 100% from β-carotene [60] or that energy transfer from xanthophylls to Chl *a* takes place at 100% transfer efficiency [61]. More recent detailed studies carried out on isolated trimers of LHCII from *Arabidopsis thaliana* using femtosecond fluorescence upconversion method showed that 56% of absorbed energy is transferred from carotenoids to Chl via the carotenoid S_2 state, and about 20% is transferred through the S_1 state [62,63].

In our pigment analysis, anthocyanins were not detected to be present. Most carotenoids were bound in PSI and PSII complexes with very little forming a band of free pigments. This means that a part of the structural carotenoids of the photosynthetic pigment–protein complexes do not transfer excitation to chlorophylls, and are thus not "accessory pigments". This result, obtained in intact leaves, is in line with earlier reports [35,64] showing that each LHCII binds one Car in an outer site, the so-called V1 (violaxanthin) binding site. This Car is unable to transfer excitation to Chls, being used as a reserve of violaxanthin for the synthesis of zeaxanthin in the xanthophyll cycle. Thus, 3 Cars in LHCII have about 80% efficiency in Car → Chl *a* transfer, 1 Car has 0% efficiency, being purely a screening pigment. The screening of 30% of blue light by photosynthetically inactive pigments is most clearly indicated in Fig. 10, where the sum of the photosynthetically active absorption cross-sections $a_{II} + a_I$ drops down to 0.7 between 450 and 500 nm. Thus, though the weakness of PSI in the blue spectral range (absorption minimum of Chl *a*) could be partially compensated for by excitation transfer from a part of carotenoids, the remaining carotenoids just screen the blue light. Physiologically this may help to avoid photoinhibition, which is particularly severe in blue light [65].

4.3. Spectrum of the quantum yields Y_{II}/Y_I

An important result of this work is the strongly conserved spectral distribution of the ratio of PSII/PSI quantum yields among broadleaf plant species (Fig. 9). If our optical measurements may seem unreliable, then Fig. 3 directly confirms that PSII activity was closely balanced with PSI activity only at wavelengths <450, 500–530 and 630 nm, but PSII was overexcited at other wavelengths under our experimental conditions. The red maximum of PSII excitation at 646 nm is followed by the "red drop" at longer wavelengths. Other characteristic maxima in PSII excitation are located at 470–490 and rather widely between 540–590 nm. The minima of PSII excitation are in the extreme blue of 397–446 nm, plus two narrow bands, one at 518 and the other at 629 nm. As a result of this spectral imbalance the Y_{II}/Y_I ratio oscillates between 1.0 and 1.6 over the wavelength range from 400 to 680 nm. Such a conserved spectral pattern of partitioning excitation between PSII and PSI confirms that the antenna systems are under strong genetic control, i.e., the number of the Lhcb and Lhca units per photosystem core is rather constant, as are the relative abundances of the PSII and PSI super-complexes, though absolute numbers per leaf area unit may vary [66–69]. Moreover, the stoichiometry of PSII to PSI reaction centers in leaf segments from spinach, cucumber and tobacco, all grown in moderate light, was recently determined by two different approaches (electrochromic signal and electron paramagnetic resonance) and gave similar PSII/PSI ratio >1 [50]. All these results are consistent with the constant Chl *a*/*b* ratio (around 3.2–3.5) measured in several plant species upon growth in full sun [70]. Considering also the data in Table 1 (Introduction), our results indicating a relatively large total PSII antenna (absorption cross-section) in leaves are consistent with the PSII/PSI ratio significantly exceeding unity – as obtained from our analysis – and/or dominating PSII composition of C2S2M2L2 in our leaves, as expected in State 1, where the loosely bound (L) LHCII trimer is attached to PSII.

Contrary to the visible part of the spectrum, where PSII is dominating, PSI is strongly dominating in the far-red part of the spectrum >690 nm. Fig. 12 illustrates the importance of far-red light for plant growth, which successively compensates for the backlog of PSI activity in the visible part of the natural sunlight. The more pronounced is the necessity for additional incandescent (far-red) illumination under gas discharge and luminescent lamps, usually poor of far-red.

In this work we pre-illuminated the leaves with PSI light, facilitating the attachment of LHC to PSII (State 1, [25,26].). The movement of one LHCII from PSII in State 1 to PSI in State 2 [71] would shift the points of Y_{II}/Y_I vertically in Fig. 9, such that the maxima of over-excitation of PSII would decrease and PSI would become over-excited with respect to PSII at wavelengths where it is equally excited in State 1 [72]. It will be the object of further research to show how much state transitions can actually regulate the spectral Y_{II}/Y_I ratio in intact leaves.

4.4. Temporal kinetics of electron transport

Along with the quantum yields of both photosystems, these measurements produced also novel information about the temporal kinetics

of inter-photosystem electron transport in intact leaves. Using the 810-nm signal we recorded the movement of electrons from PSII to PSI after flash-excitation of the photosystems. During the initial 2 ms after the flash virtually no electrons passed through the inter-photosystem chain (Fig. 5). Subsequently, the number of electrons arriving at P700 increased mono-exponentially with a time constant of 12 ms at the leaf temperature of 22 °C (Fig. 6). The mono-exponential process characterizes the turnover of a single rate-limiting chemical reaction—most likely the Q-cycle of the Cyt b_6f complex. It means that cytochromes *b* of the Cyt b_6f complex were suitably pre-reduced during the preconditioning light, to ensure the transfer of both electrons from PQH_2 to the donor side of PSI through the Q-cycle. Considering that our low-intensity flashes caused the release of a single PQH_2 molecule from only 5% of PSII, the recorded P700 reduction rate represented the diffusional and Q-cycle processes involved in the processing of a single PQH_2 molecule. With a single PQH_2 molecule as substrate the Q-cycle rate of $(12\ \text{ms})^{-1}$ was only about a half slower than the typical maximum rate of electron transfer through Cyt b_6f with maximum PQH_2 concentration of about 6 PQH_2 per PSII [73,74]. Thus, the kinetics of PQH_2 oxidation by Cyt b_6f are rather close to zero-order saturation at any realistic PQH_2 concentration, beginning from 0.05 PQH_2 per PSII. Our result also shows that in intact leaves the major rate-limiting step in inter-photosystem electron transport is not diffusion of plastoquinol, but its oxidation in the Q-cycle. Assuming that the initial sigmoidal part of the curve characterizes the release of the PQH_2 molecule from PSII (1.6 ms, [29]), plus the diffusional delay, we see that diffusion of PQ from PSII to Cyt b_6f is still much faster ($2 - 1.6 = 0.4$ ms) than the Q-cycle (12 ms). The short <1 ms diffusion time and exponentially increasing probability of the PQH_2 oxidation reaction in time do not reveal significant heterogeneities in inter-photosystem electron transport, e.g. such as percolation, resulting in domains with significantly different PQ/PSII ratio and largely variable diffusion time between the grana and stroma thylakoids [75–78].

Acknowledgement

A.L., V.O. and H.E. were supported by the Targeted Financing Theme SF0180045s08 from Estonian Ministry of Education and Science and Grants 8283 and 8344 from the Estonian Science Foundation. L.D. thanks Dr. Stefano Cazzaniga (University of Verona) for skilful technical assistance. We appreciate the advice by Dr. R. Peterson (The Connecticut Agricultural Experiment Station) in writing the manuscript.

References

[1] A. Melis, Excitation energy transfer: functional and dynamic aspects of *lhc* (*cab*) proteins, in: D.R. Ort, C.F. Yocum (Eds.), Advances in Photosynthesis, 4: Oxygenic Photosynthesis: The Light Reactions, Kluwer Academic Publishers, Dordrecht, 1996, pp. 523–538.
[2] L. Dietzel, K. Bräutigam, S. Steiner, K. Schüffler, B. Lepetit, B. Grimm, M.A. Schöttler, T. Pfannschmidt, Photosystem II supercomplex remodeling serves as an entry mechanism for state transitions in *Arabidopsis*, Plant Cell 23 (2011) 2964–2977.
[3] R.J. Strasser, W.L. Butler, Fluorescence emission spectra of photosystem I, photosystem II and the light-harvesting chlorophyll a/b complex of higher plants, Biochim. Biophys. Acta 462 (1977) 295–306.
[4] A. Pagano, G. Cinque, R. Bassi, *In vitro* reconstitution of the recombinant photosystem II light-harvesting complex CP24 and its spectroscopic characterization, J. Biol. Chem. 273 (1998) 17154–17165.
[5] Z. Liu, H. Yan, K. Wang, T. Kuang, J. Zhang, L. Gui, X. An, W. Chang, Crystal structure of spinach major light-harvesting complex at 2.72 Å resolution, Nature 428 (2004) 287–292.
[6] A. Amunts, O. Drory, N. Nelson, The structure of a plant photosystem I supercomplex at 3.4 Å resolution, Nature 447 (2007) 58–63.
[7] M. Ballotari, L. Dall'Osto, T. Morosinotto, R. Bassi, Contrasting behaviour of higher plant photosystem I and II antenna systems during acclimation, J. Biol. Chem. 282 (2007) 8947–8958.
[8] S. Caffarri, F. Passarini, R. Bassi, R. Croce, A specific binding site for neoxanthin in the monomeric antenna proteins CP26 and CP29 of photosystem II, FEBS Lett. 581 (2007) 4704–4710.
[9] P.E. Jensen, R. Bassi, E.J. Boekema, J.P. Dekker, S. Jansson, D. Leister, C. Robinson, H.V. Scheller, Structure, function and regulation of plant photosystem I, Biochim. Biophys. Acta 1767 (2007) 335–352.
[10] M. Mozzo, F. Passarini, R. Bassi, H. van Amerongen, R. Croce, Photoprotection in higher plants: the putative quenching site is conserved in all outer light-harvesting complexes of photosystem II, Biochim. Biophys. Acta 1777 (2008) 1263–1267.
[11] T. Barros, W. Kühlbrandt, Crystallization, structure and function of plant light-harvesting complex II, Biochim. Biophys. Acta 1787 (2009) 753–772.
[12] E. Wientjes, G.T. Oostergetel, S. Jansson, E.J. Boekema, R. Croce, The role of Lhca complexes in the supramolecular organization of higher plant photosystem I, J. Biol. Chem. 284 (2009) 7803–7810.
[13] A. Amunts, H. Toporik, A. Borovikova, N. Nelson, Structure determination and improved model of plant photosystem I, J. Biol. Chem. 285 (2010) 3478–3486.
[14] X. Pan, M. Li, T. Wan, L. Wang, C. Jia, Z. Hou, X. Zhao, J. Zhang, W. Chang, Structural insights into energy regulation of light-harvesting complex CP29 from spinach, Nat. Struct. Mol. Biol. 18 (2011) 309–315.
[15] Y. Umena, K. Kawakami, J.-R. Shen, N. Kamiya, Crystal structure of oxygen-evolving photosystem II at a resolution of 1.9 Å, Nature 473 (2011) 55–61.
[16] E. Wientjes, R. Croce, The light-harvesting complexes of higher-plant photosystem I: Lhca1/4 and Lhca2/3 form two red-emitting heterodimers, Biochem. J. 433 (2011) 477–485.
[17] S.W. Hogewoning, E. Wientjes, P. Douwstra, G. Trouwborst, W. van Ieperen, R. Croce, J. Harbinson, Photosynthetic quantum yield dynamics: from photosystems to leaves, Plant Cell 24 (2012) 1921–1935.
[18] J.R. Evans, A quantitative analysis of light distribution between the two photosystems, considering variation in both the relative amounts of the chlorophyll–protein complexes and the spectral quality of light, Photobiochem. Photobiophys. 10 (1986) 135–147.
[19] R. Emerson, The quantum yield of photosynthesis, Annu. Rev. Plant Physiol. 9 (1958) 1–24.
[20] R. Emerson, C.M. Lewis, The dependence of quantum yield of *Chlorella* photosynthesis on wave length of light, Am. J. Bot. 30 (1943) 165–178.
[21] K.J. McCree, The action spectrum, absorptance and quantum yield of photosynthesis in crop plants, Agric. Meteorol. 9 (1972) 191–216.
[22] K. Inada, Action spectra for photosynthesis in higher plants, Plant Cell Physiol. (1976) 355–365.
[23] J.R. Evans, The dependence of quantum yield on wavelength and growth irradiance, Aust. J. Plant Physiol. 14 (1987) 69–79.
[24] N. Murata, Fluorescence of chlorophyll in photosynthetic systems IV. Induction of various emissions at low temperatures, Biochim. Biophys. Acta 162 (1968) 106–121.
[25] D.C. Fork, The control by state transitions of the distribution of excitation energy in photosynthesis, Annu. Rev. Plant Physiol. 37 (1986) 335–361.
[26] J.F. Allen, State transition—a question of balance, Science 299 (2003) 1530–1532.
[27] R. Emerson, C.R. Lewis, The photosynthetic efficiency of phycocyanin in *Chroococcus*, and the problem of carotenoid participation in photosynthesis, J. Gen. Physiol. (March 20 1942) 579–595.
[28] H. Eichelmann, V. Oja, R.B. Peterson, A. Laisk, The rate of nitrite reduction in leaves as indicated by O_2 and CO_2 exchange during photosynthesis, J. Exp. Bot. 62 (2011) 2205–2215.
[29] V. Oja, H. Eichelmann, A. Laisk, Oxygen evolution from single- and multiple-turnover light pulses: temporal kinetics of electron transport through PSII in sunflower leaves, Photosynth. Res. 110 (2011) 99–109.
[30] A. Laisk, V. Oja, H. Eichelmann, Kinetics of leaf oxygen uptake represent in planta activities of respiratory electron transport and terminal oxidases, Physiol. Plant. 131 (2007) 1–9.
[31] V. Oja, H. Eichelmann, A. Anijalg, H. Rämma, A. Laisk, Equilibrium or disequilibrium? A dual-wavelength investigation of photosystem I donors, Photosynth. Res. 103 (2010) 153–166.
[32] V. Oja, H. Eichelmann, R.B. Peterson, B. Rasulov, A. Laisk, Decyphering the 820 nm signal: redox state of donor side and quantum yield of photosystem I in leaves, Photosynth. Res. 78 (2003) 1–15.
[33] E. Talts, V. Oja, H. Rämma, B. Rasulov, A. Anijalg, A. Laisk, Dark inactivation of ferredoxin-NADP reductase and cyclic electron flow under far-red light in sunflower leaves, Photosynth. Res. 94 (2007) 109–120.
[34] A.P. Casazza, D. Tarantino, C. Soave, Preparation and functional characterization of thylakoids from *Arabidopsis thaliana*, Photosynth. Res. 68 (2001) 175–180.
[35] S. Caffarri, R. Croce, J. Breton, R. Bassi, The major antenna complex of photosystem II has a xanthophyll binding site not involved in light harvesting, J. Biol. Chem. 276 (2001) 35924–35933.
[36] V. Oja, I. Bichele, K. Hüve, B. Rasulov, A. Laisk, Reductive titration of photosystem I and differential extinction coefficient of $P700^+$ at 810–950 nm in leaves, Biochim. Biophys. Acta 1658 (2004) 225–234.
[37] N. Bukhov, R. Carpentier, Alternative photosystem I-driven electron transport routes: mechanisms and functions, Photosynth. Res. 82 (2004) 17–33.
[38] A. Laisk, E. Talts, V. Oja, H. Eichelmann, R. Peterson, Fast cyclic electron transport around photosystem I in leaves under far-red light: a proton-uncoupled pathway? Photosynth. Res. 103 (2010) 79–95.
[39] B. Demmig, O. Bjorkman, Comparison of the effect of excessive light on chlorophyll fluorescence (77 K) and photon yield of O_2 evolution in higher plants, Planta 171 (1987) 171–184.
[40] J. Ehleringer, O. Björkman, Quantum yields for CO_2 uptake in C_3 and C_4 plants. Dependence on temperature, CO_2 and O_2 concentration, Plant Physiol. 59 (1977) 86–90.
[41] R.E. Sharp, M.A. Matthews, J.S. Boyer, Kok effect and the quantum yield of photosynthesis. Light partially inhibits dark respiration, Plant Physiol. 75 (1984) 95–101.
[42] J. Ehleringer, R.W. Pearcy, Variation in quantum yield for CO_2 uptake among C_3 and C_4 plants, Plant Physiol. 73 (1983) 555–559.

[43] S.P. Long, W.F. Postl, H.R. Bolhar-Nordenkampf, Quantum yields for uptake of carbon dioxide in C_3 vascular plants of contrasting habitats and taxonomic groupings, Planta 189 (1993) 226–234.
[44] H. Eichelmann, A. Laisk, Cooperation of photosystems II and I in leaves as analysed by simultaneous measurements of chlorophyll fluorescence and transmittance at 800 nm, Plant Cell Physiol. 41 (2000) 138–147.
[45] H. Pettai, V. Oja, A. Freiberg, A. Laisk, Photosynthetic activity of far-red light in green plants, Biochim. Biophys. Acta 1708 (2005) 311–321.
[46] G. Noctor, C.H. Foyer, Homeostasis of adenylate status during photosynthesis in a fluctuating environment, J. Exp. Bot. 51 (2000) 347–356.
[47] J.-M. Hou, V.A. Boichenko, Y.-C. Wang, P.R. Chitnis, D. Mauzerall, Thermodynamics of electron transfer in oxygenic photosynthetic reaction centers: a pulsed photoacoustic study of electron transfer in photosystem I reveals a similarity to bacterial reaction centers in both volume change and entropy, Biochemistry 40 (2001) 7109–7116.
[48] E. Pfündel, Estimating the contribution of photosystem I to total leaf chlorophyll fluorescence, Photosynth. Res. 56 (1998) 185–195.
[49] R. Peterson, V. Oja, A. Laisk, Chlorophyll fluorescence at 680 and 730 nm and its relationship to photosynthesis, Photosynth. Res. 70 (2001) 185–196.
[50] D.-Y. Fan, A.B. Hope, P.J. Smith, H. Jia, R.J. Pace, J.M. Anderson, W.S. Chow, The stoichiometry of the two photosystems in higher plants revisited, Biochim. Biophys. Acta 1767 (2007) 1064–1072.
[51] A. Laisk, H. Eichelmann, V. Oja, Oxygen evolution and chlorophyll fluorescence from multiple turnover light pulses: charge recombination in photosystem II in sunflower leaves, Photosynth. Res. 113 (2012) 145–155.
[52] A. Laisk, V. Oja, Thermal phase and excitonic connectivity in fluorescence induction, Photosynth. Res. (2013), http://dx.doi.org/10.1007/s11120-013-9915-1.
[53] U. Schreiber, Assessment of maximal fluorescence yield. Donor-side dependent quenching and Q_B-quenching, in: O. Van Kooten, J. Snel (Eds.), Plant Spectrophotometry: Applications and Basic Research, Rozenberg, Amsterdam, 2002, pp. 23–47.
[54] G. Renger, B. Hanssum, Oxygen detection in biological systems, Photosynth. Res. 102 (2009) 487–498.
[55] M.R. Badger, T.D. Sharkey, S. von Caemmerer, The relationship between steady-state gas exchange of bean leaves and the levels of carbon-reduction-cycle intermediates, Planta 160 (1984) 305–313.
[56] V. Oja, H. Eichelmann, A. Laisk, The size of the lumenal proton pool in leaves during induction and steady-state photosynthesis, Photosynth. Res. 110 (2011) 73–88.
[57] V. Oja, A. Laisk, Oxygen yield from single turnover flashes in leaves: non-photochemical excitation quenching and the number of active PSII, Biochim. Biophys. Acta 1460 (2000) 291–301.
[58] R. Emerson, C.M. Lewis, The photosynthetic efficiency of phycocyanin in *Chroococcus*, and the problem of carotenoid participation in photosynthesis, J. Gen. Physiol. (1942) 579–595.
[59] L.N.M. Duysens, Transfer of Excitation Energy in Photosynthesis, Dissertation The State University, Utrecht, 1952.
[60] J.C. Goedheer, Energy transfer from carotenoids to chlorophyll in blue-green, red and green algae and greening bean leaves, Biochim. Biophys. Acta 172 (1969) 252–265.
[61] D. Siefermann-Harms, H. Ninnemann, Pigment organization in the light-harvesting chlorophyll-a/b protein complex of lettuce chloroplasts. Evidence obtasined from protection of the chlorophylls against proton attack and from excitation energy transfer, Photochem. Photobiol. 35 (1982) 719–731.
[62] R. Croce, M.G. Müller, R. Bassi, A.R. Holzwarth, Carotenoid-to-chlorophyll energy transfer in recombinant major light-harvesting complex (LHCII) of higher plants. I. Femtosecond transient absorption measurements, Biophys. J. 80 (2001) 901–915.
[63] N.E. Holt, J.T.M. Kennis, L. Dall'Osto, R. Bassi, G.R. Fleming, Carotenoid to chlorophyll energy transfer in light harvesting complex II from *Arabidopsis thaliana* probed by femtosecond fluorescence upconversion, Chem. Phys. Lett. 379 (2003) 305–313.
[64] L. Dall'Osto, S. Cazzaniga, H. North, A. Marion-Poll, R. Bassi, The *Arabidopsis* aba4-1 mutant reveals a specific function for neoxanthin in protection against photooxidative stress, Plant Cell 19 (2007) 1048–1067.
[65] U. Schreiber, C. Klughammer, Wavelength-dependent photodamage to *Chlorella* investigated with a new type of multi-color PAM chlorophyll fluorometer, Photosynth. Res. 114 (2013) 165–177.
[66] M. Ballottari, C. Govoni, S. Caffarri, T. Morosinotto, Stoichiometry of LHCI antenna polypeptides and characterization of gap and linker pigments in higher plants photosystem I, Eur. J. Biochem. 271 (2004) 4659–4665.
[67] M. Ballottari, L. Dall'Osto, T. Morosinotto, R. Bassi, Contrasting behaviour of higher plant photosystem I and II antenna systems during acclimation, JBC Papers, 2007, http://dx.doi.org/10.1074/jbc.M606417200.
[68] S. Caffarri, R. Croce, L. Cattivelli, R. Bassi, A look within LHCII: differential analysis of the Lhcb1-3 complexes building the major trimeric antenna complexes of higher-plant photosynthesis, Biochemistry 43 (2004) 9467–9476.
[69] M. Fuciman, M.M. Enriquez, T. Polivka, L. Dall'Osto, R. Bassi, H.A. Frank, Role of xanthophylls in light harvesting in green plants: a spectroscopic investigation of mutant Lhcb pigment–protein complexes, J. Phys. Chem. B 116 (2012) 3834–3849.
[70] B. Demmig-Adams, Survey of thermal energy dissipation and pigment composition in sun and shade leaves, Plant Cell Physiol. 39 (1998) 474–482.
[71] P. Galka, A. Santabarbara, T.T.H. Khuong, H. Degand, P. Morsomme, R.C. Jennings, E.J. Boekema, S. Caffarri, Functional analyses of the plant photosystem I-light-harvesting complex II supercomplex reveal that light-harvesting complex II loosely bound to photosystem II is a very efficient antenna for photosystem I in state II, Plant Cell 24 (2012) 2963–2978.
[72] O. Canaani, S. Malkin, Distribution of light excitation in an intact leaf between the two photosystems of photosynthesis. Changes in absorption cross-sections following state1–state2 transitions, Biochim. Biophys. Acta 766 (1984) 512–524.
[73] U. Siggel, The control of electron transport by two pH-sensitive sites, in: M. Avron (Ed.), Proc. 3-Rd Internat. Congr. on Photosynth, Elsevier, Amsterdam, 1974, pp. 645–654.
[74] A. Laisk, V. Oja, Range of the photosynthetic control of postillumination P700 reduction rate in sunflower leaves, Photosynth. Res. 39 (1994) 39–50.
[75] P. Joliot, J. Lavergne, D. Béal, Plastoquinone compartmentation in chloroplasts. I. Evidence for domains with different rates of photo-reduction, Biochim. Biophys. Acta 1101 (1992) 1–12.
[76] P. Joliot, A. Joliot, Electron transfer between photosystem II and the cytochrome b/f complex: mechanistic and structural implications, Biochim. Biophys. Acta 1102 (1992) 53–61.
[77] I.G. Tremmel, H. Kirchhoff, E. Weis, G.D. Farquhar, Dependence of plastoquinol diffusion on the shape, size, and density of integral thylakoid proteins, Biochim. Biophys. Acta 1607 (2003) 97–109.
[78] H. Kirchhoff, S. Horstmann, E. Weis, Control of the photosynthetic electron transport by PQ diffusion microdomains in thylakoids of higher plants, Biochim. Biophys. Acta 1459 (2000) 148–168.